2954 *Inorg. Chem.* **2010**, *49*, 2954–2959
DOI: 10.1021/ic902498p

Inorganic Chemistry
Article

Synthesis and Properties of Tetracyanamidosilicates ARE[Si$(CN_2)_4$]

Jochen Glaser,[†] Helga Bettentrup,[‡] Thomas Jüstel,*[,‡] and H.-Jürgen Meyer*[,†]

[†]*Institut für Anorganische Chemie, Universität Tübingen, Ob dem Himmelreich 7, D-72074 Tübingen, Germany, and* [‡]*Fachhochschule Münster, Labor für Angewandte Materialwissenschaft, Stegerwaldstrasse 39, D-48565 Steinfurt, Germany*

Received December 16, 2009

Tetracyanamidosilicates of the type ARE[Si$(CN_2)_4$] with A = K, Rb, and Cs and RE = Y and La−Lu have been prepared by a solid-state metathesis reaction. The potassium compounds with RE = La−Gd crystallize orthorhombically in the space group $P2_12_12$. Rubidium as well as cesium compounds crystallize tetragonally in the space group $I\bar{4}$. The luminescent properties of ARE[Si$(CN_2)_4$]:Ln compounds with RE = Y, La, and Gd doped with 5 mol % Ln = Ce, Eu, or Tb were investigated. Temperature-dependent magnetic susceptibilities were measured for KGd[Si$(CN_2)_4$]. The value of the magnetic moment is 7.3 μ_B/Gd^{3+} ion, which is in line with the expected value for the [Xe]$4f^7$ configuration of Gd^{3+}.

Introduction

Since the invention of blue-emitting InGaN light-emitting diodes (LEDs),[1] there is a tremendous interest in the development of white LEDs for general lighting purposes. The main advantages of the application of LEDs in general lighting are their long lifetime, flexibility, and high luminous efficiency, which recently achieved 250 lm/W.[2]

Presently applied white high-power LEDs basically consist of a blue-emitting InGaN chip coated by a yellow-emitting luminescent material, mostly $Y_3Al_5O_{12}$:Ce (YAG:Ce), to obtain white light due to additive color mixing. This yields cool white LEDs with high color temperatures T_c above 4000 K, which do not meet the requirements for ambient lighting. To obtain warm-white LEDs (T_c < 4000 K), the application of an additional red phosphor is required. Presently available warm-white LEDs achieve this by employment of a broad-band red emitter, which is mostly (Ca,Sr)S:Eu,[3] (Ca,Sr)$AlSiN_3$:Eu,[4] or (Ca,Sr,Ba)$_2Si_5N_8$:Eu,[5] although this is at the cost of the lumen equivalent. Consequently, the luminous efficiency of white LEDs comprising YAG:Ce decreases by about 50%, once a broad-band Eu^{2+} phosphor is applied as an additional red emitter. This strong decrease in the luminous efficiency is caused by the low lumen equivalent of broad-band red-emitting phosphors because of tailing of the emission band into the hardly visible near-IR range.

Red-emitting phosphors for warm-white LEDs must show a strong absorption at the emission maximum of the LED die and high quantum efficiency, even at 150 °C, i.e. at the temperature of an operating LED chip. Even though Eu^{3+}-activated phosphors do not show strong absorption in the blue spectral range, their high efficiency, high lumen equivalent, and superior photochemical and thermal stability justify the intense search for a Eu^{3+} phosphor as a red-emitting luminescent material for LEDs.

The recent development of efficient near-UV LEDs enables the development of white LEDs based on a platform concept using a 370−400 nm emitting InGaN die and a trichromatic phosphor blend because it is used in fluorescent lamps. However, this requires the availability of efficient green- and blue-emitting phosphors, which are efficiently luminescent upon excitation in the near-UV. Suitable activator ions for phosphors showing blue and green emission are Ce^{3+} and Tb^{3+}.

The novel tetracyanamidosilicates of type ARE[Si$(CN_2)_4$] with A = K, Rb, and Cs and RE = La, Ce, Pr, Nd, Sm, Gd, Tb, Dy, Ho, Er, Tm, Yb, Lu, and Y described in this paper are of high interest as host lattices for luminescent ions, such as Ce^{3+}, Eu^{3+}, and Tb^{3+}. This interest is driven by the coordination geometry and covalent interaction of the rare-earth ions in host lattices with highly polarizable anions. This justifies the expectation that the charge-transfer (CT) level of Eu^{3+} and the 4f5d level of Ce^{3+} or Tb^{3+} are located at such a low energy that the energy of these levels overlap with the energy of the incident photons from a blue- or near-UV-emitting LED die.

Experimental Section

Preparation of ARE[Si$(CN_2)_4$] (A = K, Rb, Cs; RE = Y, La, Pr, Nd, Sm, Gd−Lu). All manipulations of the starting materials

*To whom correspondence should be addressed. E-mail: tj@fh-muenster.de (T.J.), juergen.meyer@uni-tuebingen.de (H.-J.M.).

(1) Nakamura, S.; Mukai, T.; Senoh, M. *Appl. Phys. Lett.* **1994**, *64*, 1687–1689.
(2) Nichia Ltd., Internet publication, Feb 2, **2009**.
(3) Jüstel, T.; Schmidt, P. J.; Müller, G. O.; Müller-Mach, R. U.S. Patent 0,006,702, 2003.
(4) Kijima, N.; Piao, X.; Machida, K.; Horikawa, T.; Hanzawa, H.; Shimomura, Y. *Chem. Mater.* **2007**, *19*, 4592–4599.
(5) Yamada, M.; Naitou, T.; Izuno, K.; Tamaki, H.; Murazaki, Y.; Kameshima, M.; Mukai, T. *Jpn. J. Appl. Phys., Part II: Lett.* **2003**, *42*, L20–23.

 Published on Web 02/16/2010

were carried out in a glovebox under an argon atmosphere. Rare-earth trichlorides ($RECl_3$; ABCR, 99.9%) were mixed thoroughly in a mortar together with A_2SiF_6 (A = K, Chempur, 99%; A = Rb, Cs, see below) and $Li_2(CN_2)$ (see the preparation below). Doped samples of the yttrium, lanthanum, and gadolinium compounds were prepared by the substitution of 5 mol % of yttrium, lanthanum, or gadolinium trichloride with cerium, europium, or terbium trichloride, respectively. The mixtures were placed in dry quartz glass ampules, which were evacuated and sealed. The ampules were heated in a furnace to 550 °C (5 °C/min), held at this temperature for 2 days, and then cooled to room temperature by switching off the furnace. The glass ampules with the reaction products were opened in air. The products were washed with water five times to remove LiF and other soluble byproducts, rinsed twice with ethanol, and dried at 100 °C in air.

Preparation of H_2SiF_6. An aqueous H_2SiF_6 solution was prepared in a polyethylene beaker by dissolving SiO_2 (99.9%, −325 mesh, Ventron) in an aqueous HF solution (38%, J. T. Baker).

Preparation of Hexafluorosilicates. Hexafluorosilicates of rubidium and cesium were precipitated from an aqueous solution of H_2SiF_6 with appropriate amounts of RbF and CsF (Merck, Selectipur), filtered off, washed with cold water, rinsed with ethanol, and dried in air. The X-ray diffraction (XRD) patterns of the products showed only lines of Rb_2SiF_6 and Cs_2SiF_6, respectively.

Preparation of $Li_2(CN_2)$. Lithium carbodiimide was made from Li_3N (700 mg, 99.4%, Alfa Aesar) and melamine (1400 mg, 99+%, Aldrich). The mixture was placed in a silver boat and first heated in a tubular furnace under dry dinitrogen to 270 °C (10 °C/min), then to 330 °C (1 °C/min), and finally to 600 °C (10 °C/min). After cooling to room temperature, the mixture was ground together with 150 mg of melamine and heated again to 600 °C (10 °C/min), held at this temperature for 30 min, and cooled to room temperature. The reaction product was pure $Li_2(CN_2)$ according to powder XRD.

Powder XRD. The XRD patterns of all reaction products were collected with a powder diffractometer (Stoe STADI-P, Ge monochromator) using Cu $K\alpha_1$ radiation. For calculation of the lattice parameters, reflections of the potassium compounds (La−Gd) were indexed isotypically to $KLa[Si(CN_2)_4]$[6] with the aid of the program package *WinXPow*.[7] The powder XRD patterns of the rubidium and cesium compounds were indexed isotypically to $RbLa[Si(CN_2)_4]$. Results of the lattice parameter determinations are given in Table 1.

Luminescence Spectroscopy. Excitation and emission spectra were collected with a fluorescence spectrometer FLS920 (Edinburgh Instruments) equipped with a 450 W ozone-free xenon discharge lamp (OSRAM) and a sample chamber installed with a mirror optic for powder samples. For detection, a R2658P single-photon-counting photomultiplier tube (Hamamatsu) was used. All luminescence spectra were recorded with a spectral resolution of 1 nm, a dwell time of 0.2 s in 1 nm steps, and three repeats.

Magnetic Measurement. The magnetic susceptibility of $KGd[Si(CN_2)_4]$ was measured by using a SQUID magnetometer (Quantum Design, MPMS) in the temperature range from 300 to 1.8 K.

Results and Discussion

Synthesis, Structure, and Magnetism. A whole series of rare-earth tetracyanamidosilicate compounds having the composition $ARE[Si(CN_2)_4]$ was prepared by multilateral solid-state metathesis reactions, following the reaction equation

$$RECl_3 + A_2[SiF_6] + 4Li_2(CN_2) \rightarrow ARE[Si(CN_2)_4] + 2LiCl + 6LiF + ACl$$

The reaction products contained the desired compounds besides the coproduced salts, which were rinsed with water. Powder XRD patterns of the potassium series were indexed isotypically to $KLa[Si(CN_2)_4]$, and those of the rubidium and cesium series were indexed isotypically to $RbLa[Si(CN_2)_4]$. Preparations of the potassium compounds with smaller rare earths were not successful because the competing quasi binary carbodiimides[8] seemed to be more stable than the tetracyanamidosilicates under conditions that we have used. As expected, the unit cell volumes of the tetracyanamidosilicates decrease with decreasing rare-earth metal ion, following the trend of the lanthanide contraction (Figure 1).

The structures of the tetracyanamidosilicates contain $[Si(CN_2)_4]^{4-}$ ions (d_{Si-N} = 1.71−1.72 Å), which can be

Table 1. Volume (V in Å^3), Lattice Parameters a, b, and c (in Å) of $ARE[Si(CN_2)_4]$ Compounds with A = K, Rb, and Cs and RE = Y and La−Lu (except Pm and Eu), and the Number N of Single Indexed Reflections

RE	a	b	c	V	N
	$KRE[Si(CN_2)_4]$, Orthorhombic, Space Group $P2_12_12$				
La	9.486(2)	7.613(2)	6.854(2)	495.0(2)	34
Ce	9.436(3)	7.586(2)	6.801(2)	486.8(3)	35
Pr	9.413(2)	7.571(2)	6.767(3)	482.3(3)	35
Nd	9.387(3)	7.561(3)	6.735(3)	478.0(4)	32
Sm	9.319(4)	7.543(3)	6.683(3)	469.7(5)	33
Gd	9.277(6)	7.522(3)	6.649(4)	464.0(6)	27
	$RbRE[Si(CN_2)_4]$, Tetragonal, Space Group $I\bar{4}$				
La	8.561(4)		6.840(4)	501.3(6)	25
Ce	8.531(3)		6.792(2)	494.3(4)	24
Pr	8.498(2)		6.755(2)	487.8(3)	27
Nd	8.473(4)		6.722(3)	482.6(5)	18
Sm	8.442(3)		6.674(2)	475.6(3)	24
Gd	8.415(3)		6.636(2)	469.9(3)	29
Tb	8.389(5)		6.611(3)	465.3(6)	23
Dy	8.371(2)		6.594(2)	462.1(3)	27
Ho	8.355(2)		6.574(1)	458.9(2)	27
Er	8.339(3)		6.559(2)	456.1(3)	29
Tm	8.326(2)		6.546(2)	453.7(3)	26
Yb	8.302(3)		6.532(3)	450.2(4)	31
Lu	8.299(3)		6.524(3)	449.3(3)	28
Y	8.360(2)		6.582(2)	456.9(3)	27
	$CsRE[Si(CN_2)_4]$, Tetragonal, Space Group $I\bar{4}$				
La	8.645(2)		6.851(2)	512.0(3)	20
Ce	8.613(1)		6.804(1)	504.7(2)	28
Pr	8.583(2)		6.766(1)	498.4(2)	30
Nd	8.568(1)		6.737(1)	494.6(2)	29
Sm	8.519(2)		6.683(2)	485.0(2)	23
Gd	8.486(2)		6.645(1)	478.5(2)	25
Tb	8.463(1)		6.623(1)	474.4(2)	27
Dy	8.445(1)		6.603(1)	471.0(2)	29
Ho	8.429(1)		6.587(1)	468.0(2)	29
Er	8.415(2)		6.570(1)	465.2(2)	31
Tm	8.398(2)		6.556(2)	462.3(2)	28
Yb	8.375(2)		6.543(2)	458.9(2)	31
Lu	8.359(2)		6.529(2)	456.2(3)	27
Y	8.430(2)		6.591(2)	468.4(3)	31

(6) Glaser, J.; Meyer, H.-J. *Angew. Chem., Int. Ed.* **2008**, *47*, 7547–7550.
(7) *WinXPow, Diffractometer Software*, version 1.10; Stoe & Cie GmbH: Darmstadt, Germany, 1997.
(8) Neukirch, M.; Tragl, S.; Meyer, H.-J. *Inorg. Chem.* **2006**, *45*, 8188–8193.

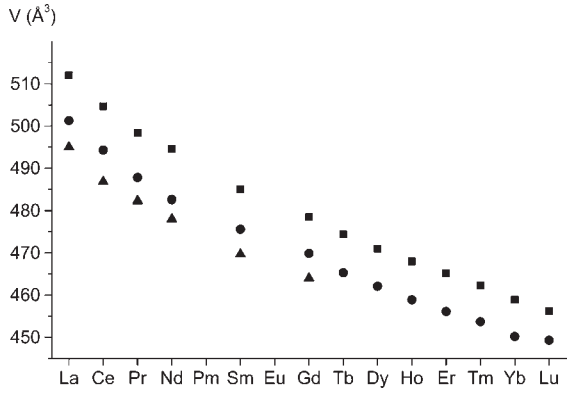

Figure 1. Unit cell volume of ARE[Si(CN$_2$)$_4$] compounds with A = K, Rb, and Cs and RE = Y and La−Lu (except Pm and Eu).

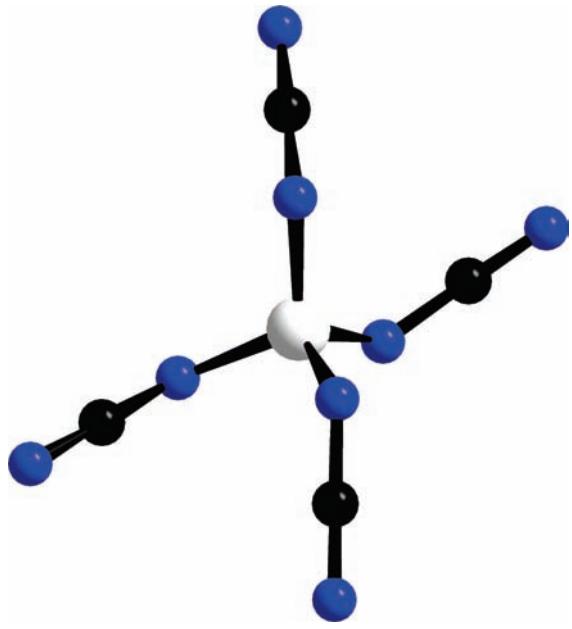

Figure 2. Tetracyanamidosilicate ion in ARE[Si(CN$_2$)$_4$] compounds with A = K, Rb, and Cs and RE = Y and La−Lu. The silicon atom is in white, the nitrogen atoms are in blue, and the carbon atoms are in black.

derived from orthosilicates when substituting the oxygen atoms by [NCN] units (Figure 2). The [NCN] units in the structures are almost linear ($\angle$N−C−N = 177−180°) but represent cyanamide ions having two clearly distinct distances, being at d_{C-N} = 1.274(9) and 1.16(1) Å in RbLa[Si(CN$_2$)$_4$], which are close to the distances obtained in the cyanamide molecule (H$_2$N−C≡N) of 1.31 and 1.15 Å.

The tetracyanamidosilicate ions are surrounded by six rare-earth metal ions forming a distorted octahedron. The rare-earth metal ions are coordinated by six anions building a distorted octahedron as well. All together, the arrangements of these groups form a three-dimensional network structure in which the silicon atoms and rare-earth metal ions form a motif related with the atom arrangements in the NaCl-type structure. The alkaline metal ions occupy half of the tetrahedral voids being created in the structure. Figure 3 (left) shows the arrangement of the potassium compound in which K^+ ions reside at comparable places like oxygen atoms do in the PbO structure. Figure 3 (right) shows the arrangement in structures containing A = Rb and Cs, where the alkaline metal ions reside at comparable places like sulfur atoms do in the ZnS structure (sphalerite).

The rare-earth ions in the structures are coordinated by eight nitrogen atoms of the tetracyanamidosilicate groups, forming a distorted trigonal dodecahedron (Figure 4). This coordination environment is due to both types of nitrogen atoms, four terminal ones and four nitrogen atoms that are bonded directly to the silicon center.

The rare-earth ions of the orthorhombic structure have a point symmetry of 2, leading to four different La−N distances {2× [2.549(6), 2.574(6), 2.621(5), and 2.690(5) Å]}. The rare-earth ions of the tetragonal structure have a point symmetry of $\bar{4}$ with two different La−N distances {4× [2.555(7) and 2.659(5)] Å}. Two different Y−O distances {4× [2.306 and 2.439 Å]} occur in $Y_3Al_5O_{12}$ as a result of the point symmetry 222 of the Y^{3+} ion in the garnet structure.

Long-range magnetic ordering is possible in similar network structures in which cations are interconnected with larger polyatomic anions such as dicyanamides $[N(CN)_2]^-$ or tricyanomethanides $[C(CN)_3]^-$ if conjugated π systems allow pathways for magnetic interactions between paramagnetic metal centers.[9] For example, compounds of the type M[N(CN)$_2$]$_2$ with divalent metal ions (M = V, Cr, Mn, Co, Ni, Cu)[10] or M[C(CN)$_3$]$_2$ (M = V, Cr, Mn, Fe, Co, Ni, Cu)[11] show antiferromagnetic interactions.

Magnetic measurements of KGd[Si(CN$_2$)$_4$] show almost perfect Curie paramagnetic behavior (Figure 5) in the temperature range from 300 to 10 K of seven unpaired electrons of the Gd^{3+} ion (μ_{exp} = 7.3 μ_B; theory, μ_{eff} = 7.9 μ_B).

Luminescence. Because the herein-described compounds show an 8-fold coordination of the rare-earth metal ions with a distorted trigonal dodecahedron, which is similar to the coordination geometry in garnets of the type $RE_3Al_5O_{12}$ (with RE = Y, Eu−Lu), one can expect luminescence spectra of a similar type. However, the different crystal-field splitting and covalent interaction might result in different spectral positions of the electronic transitions, in which 5d orbitals are involved.

Ce^{3+}-doped KLa[Si(CN$_2$)$_4$] shows deep-blue luminescence with a broad emission band at 430 nm due to the spin- and parity-allowed [Xe]5d^1 (^{2}D) to [Xe]4f^1 ($^2F_{7/2}$, $^2F_{5/2}$) interconfigurational transition of Ce^{3+} (Figure 6). The excitation spectrum monitored for the 430 nm emission band reveals two bands located at 355 and 290 nm

(9) (a) Miller, J. S.; Manson, J. L. *Acc. Chem. Res.* **2001**, *34*, 563–670. (b) Miyasaka, H.; Clerac, R.; Campos-Fernandez, C. S.; Dunbar, K. R. *Inorg. Chem.* **2001**, *40*, 1663–1671.

(10) (a) Batten, S. R.; Jensen, P.; Moubaraki, B.; Murray, K. S.; Robson, R. *Chem. Commun.* **1998**, 439–440. (b) Jensen, P.; Batten, S. R.; Fallon, G. D.; Moubaraki, B.; Murray, K. S.; Price, D. *Chem. Commun.* **1999**, 177–178. (c) Batten, S. R.; Murray, K. S. *Coord. Chem. Rev.* **2003**, *246*, 103–130. (d) Kurmoo, M.; Kepert, C. J. *New J. Chem.* **1998**, *22*, 1515–1524. (e) Manson, J. L.; Kmety, C. R.; Epstein, A. J.; Miller, J. S. *Inorg. Chem.* **1999**, *38*, 2552–2553. (f) Manson, J. L.; Kmety, C. R.; Huang, Q.; Lynn, J. W.; Bendele, G. M.; Pagola, S.; Stephens, P. W.; Liable-Sands, L. M.; Rheingold, A. L.; Epstein, A. J.; Miller, J. S. *Chem. Mater.* **1998**, *10*, 2552–2560.

(11) (a) Enemark, J. H.; Holm, R. H. *Inorg. Chem.* **1964**, *3*, 1516–1521. (b) Manson, J. L.; Ressouche, E.; Miller, J. S. *Inorg. Chem.* **2000**, *39*, 1135–1141. (c) Hoshino, H.; Iida, K.; Kawamoto, T.; Mori, T. *Inorg. Chem.* **1999**, *38*, 4229–4232. (d) Feyerherm, R.; Loose, A.; Landsgesell, S.; Manson, J. L. *Inorg. Chem.* **2004**, *43*, 6633–6639.

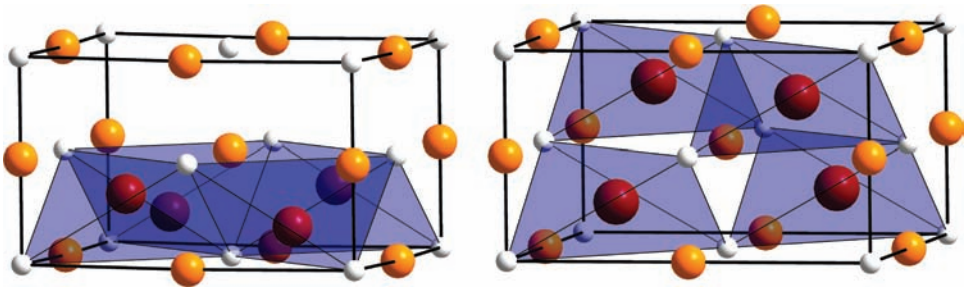

Figure 3. Simplified structures of $KLa[Si(CN_2)_4]$ (left) and $RbLa[Si(CN_2)_4]$ (right). The silicon atoms are in white, the lanthanum atoms in orange, and the alkaline metal atoms in dark red. The lines between the atoms are just guides for the eyes.

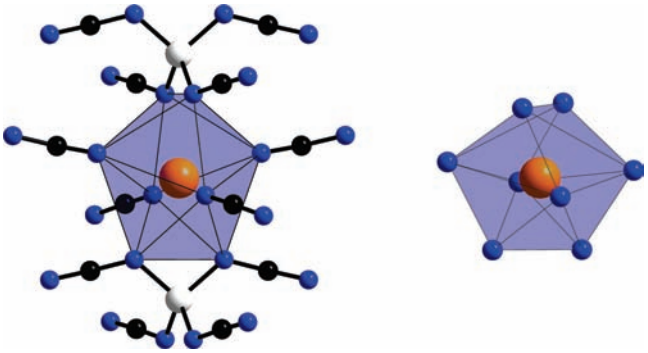

Figure 4. Trigonal-dodecahedral environments of the rare-earth ions in the structures of $ARE[Si(CN_2)_4]$ (left) and $RE_3Al_5O_{12}$ (right).

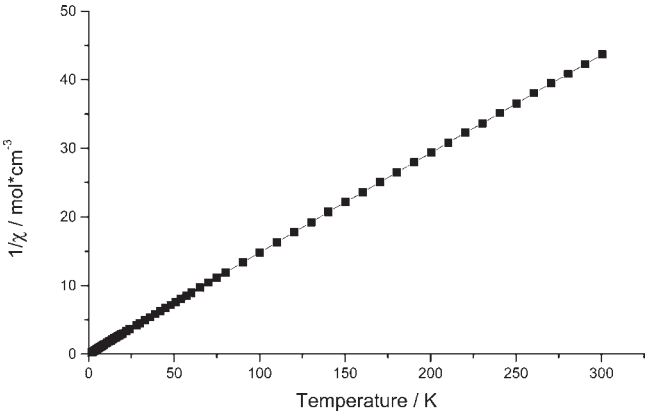

Figure 5. Magnetic susceptibility of $KGd[Si(CN_2)_4]$ projected as a $1/\chi$ vs T plot.

and a shoulder at 270 nm. Because the Ce^{3+} ions are assumed to occupy La^{3+} sites, which have distorted dodecahedral environments, the ^2D term of the Ce^{3+} $[Xe]5d^1$ excited-state configuration is expected to split into five levels by the crystal-field interaction. The fact that only three transitions are observed means that either some of the five related bands are so close to each other that they cannot be resolved or that the two missing bands are located below 250 nm.

An interesting finding is that the present material shows a more saturated blue color point than $LiYSiO_4$:Ce[12] and Y_2SiO_5:Ce, although the emission band maximum is located at almost the same spectral position. Because the latter material found even commercial application

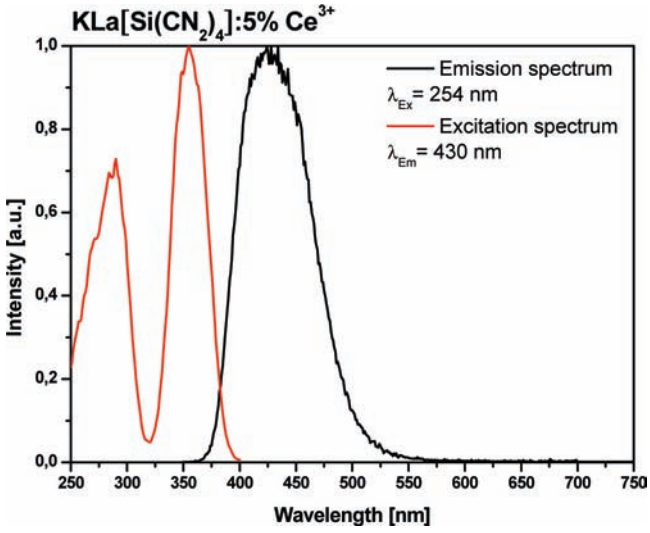

Figure 6. Excitation and emission spectra of $KLa[Si(CN_2)_4]$:5% Ce^{3+}.

as a scintillator and as a low-voltage field-emission-display phosphor,[13] our material might be of interest. The superior color point can be interpreted in view of the narrower emission band of $KLa[Si(CN_2)_4]$:Ce.

Tb^{3+}-doped $KLa[Si(CN_2)_4]$, $RbLa[Si(CN_2)_4]$ (Figure 7), and $RbGd[Si(CN_2)_4]$ (Figure 8) exhibit the typical green-yellow luminescence of Tb^{3+} as was expected for those luminescent materials, in which the $^5D_4$ to ^7F_J ($J = 0-6$) transitions dominate the spectrum, while the $^5D_3$ level is quenched because of either phonon or cross relaxation.[14] The quenching of the $^5D_3$ level of the tetracyanamidosilicates is caused by phonon relaxation because of the presence of high-energy phonons, viz., $\nu_{as}(N-C-N)$ located at 2145 cm^{-1} for $KLa[Si(NCN)_4]$, which is confirmed by our observation that samples with a rather low Tb^{3+} concentration do not show luminescence because of $^5D_3-^7F_J$ transitions (Figure 7).

From the emission spectra, which show emission lines at 487 nm ($^7F_6$), 545 nm ($^7F_5$), 586 nm ($^7F_4$), 621 nm ($^7F_3$), 648 nm ($^7F_2$), 667 nm ($^7F_1$), and 678 nm ($^7F_0$) (Figure 7), we calculated the lumen equivalent and the CIE 1931 color points (Table 2). Both values point to a low symmetry of the local site of Tb^{3+} because the $^5D_4-^7F_5$ to $^5D_4-^7F_J$ ($J = 0-4, 6$) intensity ratio is a sensitive function of the site symmetry.[14] In contrast to YBO_3:Tb, which

(12) Knitel, M. J.; Dorenbos, P.; van Eijk, C. W. E. *J. Lumin.* **1997**, *72−74*, 765–766.

(13) Lee, R. Y.; Zhang, F. L.; Penczek, J.; Wagner, B. K.; Yocom, P. N.; Summers, C. J. *J. Vac. Sci. Technol. B* **1998**, *16*, 855–857.

(14) Blasse, G.; Grabmeier, B. C. *Luminescent Materials*; Springer Verlag: Berlin, 1994.

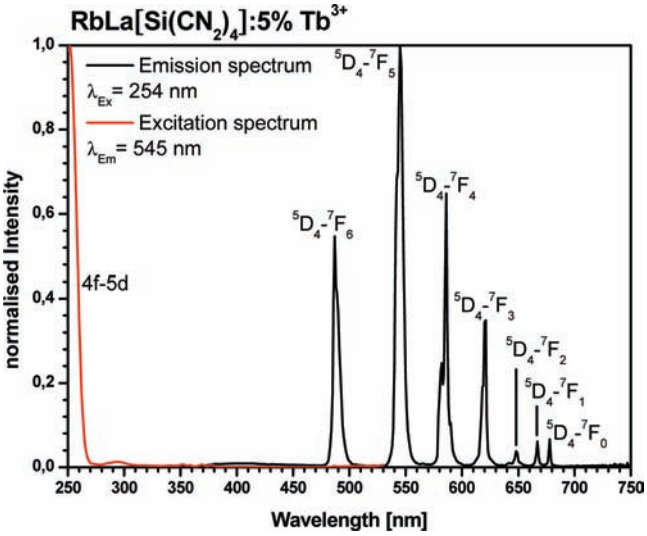

Figure 7. Excitation and emission spectra of RbLa[Si(CN$_2$)$_4$]:5% Tb^{3+}.

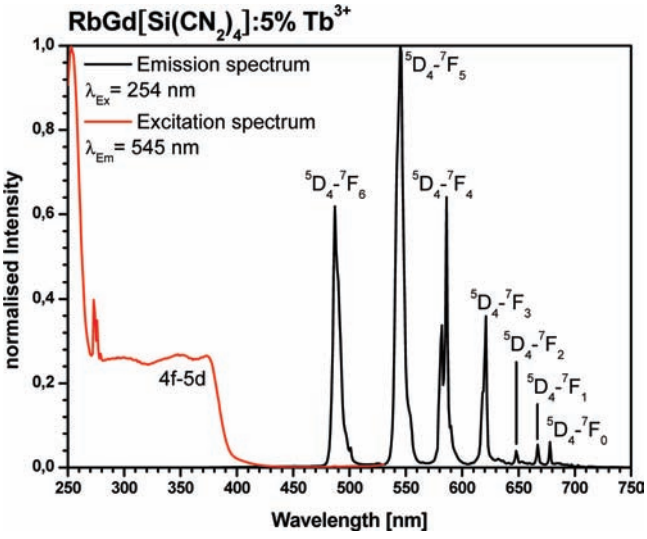

Figure 8. Excitation and emission spectra of RbGd[Si(CN$_2$)$_4$]:5% Tb^{3+}.

shows a high lumen equivalent of 530 lm/W and a high *y* value of around 0.61,[15] the herein-discussed materials are thus less suitable for lighting and display applications. However, the excitation spectra of KLa[Si(CN$_2$)$_4$]:Tb and RbLa[Si(CN$_2$)$_4$]:Tb (Figure 7) monitored for the 545 nm emission line show that the lowest crystal-field component of the [Xe]4f^{7}5d^1 configuration is located at around 250 nm, which demonstrates that the material can be efficiently excited by a low-pressure mercury discharge. Moreover, the excitation spectrum of RbGd[Si(CN$_2$)$_4$]:Tb (Figure 8) monitored for the 545 nm emission line shows an excitation line mulitplet at around 270 nm and three excitation bands at 300, 350, and 380 nm. While the excitation lines can be assigned to the ^{8}S to ^{6}I$_J$ transitions of Gd^{3+}, the broad bands are caused by the low-lying crystal-field components of the [Xe]4f^{7}5d^1 configuration. The low energy of these levels points to a much larger crystal-field splitting compared to the situation in KLa[Si(CN$_2$)$_4$]:Tb and RbLa[Si(CN$_2$)$_4$]:Tb. This might be explained by the fact that Tb^{3+} occupies in RbGd[Si(CN$_2$)$_4$] the much narrower Gd^{3+} site, yielding a stronger crystal-field splitting and covalent interaction due to lower Tb^{3+} anion distances.

(15) Kim Kwon, I.-E.; Park, C.-H.; Hwang, Y.-J.; Bae, H.-S.; Yu, B.-Y.; Pyun, C.-H.; Hong, G.-Y. *J. Alloys Compd.* **2000**, *311*, 33–39.

Table 2. CIE 1931 Color Points and Lumen Equivalents As Calculated from the Emission Spectra upon 254 or 394 nm Excitation

	CIE 1931 color coordinate		
composition	*x*	*y*	lumen equivalent (lm/W)
KLa[Si(CN$_2$)$_4$]:Ce	0.154	0.047	37
KLa[Si(CN$_2$)$_4$]:Tb	0.356	0.538	450
RbLa[Si(CN$_2$)$_4$]:Tb	0.362	0.531	443
RbGd[Si(CN$_2$)$_4$]:Tb	0.354	0.541	449
KGd[Si(CN$_2$)$_4$]:Eu	0.610	0.336	260
RbLa[Si(CN$_2$)$_4$]:Eu	0.630	0.370	287
CsGd[Si(CN$_2$)$_4$]:Eu	0.627	0.368	280
CsLa[Si(CN$_2$)$_4$]:Eu	0.624	0.371	286
CsY[Si(CN$_2$)$_4$]:Eu	0.592	0.397	303

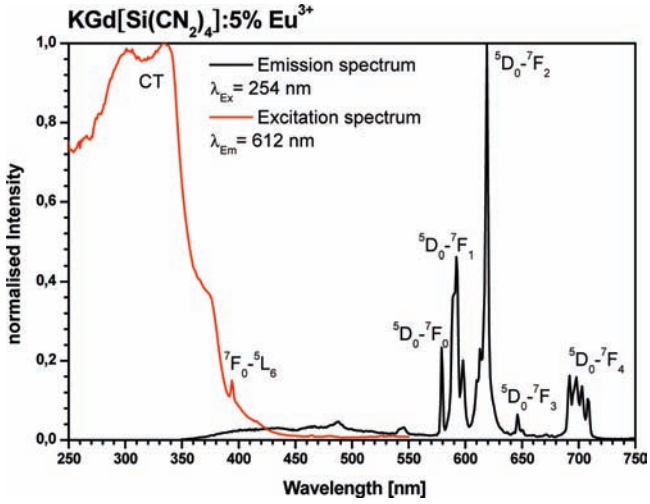

Figure 9. Excitation and emission spectra of KGd[Si(CN$_2$)$_4$]:5% Eu^{3+} (orthorhombic).

Eu^{3+}-doped KGd[Si(CN$_2$)$_4$], RbLa[Si(CN$_2$)$_4$], CsGd[Si(CN$_2$)$_4$], CsLa[Si(CN$_2$)$_4$], and CsY[Si(CN$_2$)$_4$] (Figure 9–11) exhibit orange to red luminescence upon 254 or 394 nm excitation as a result of the emission lines located between 580 and 710 nm caused by the ^{5}D$_0$ to ^{7}F$_J$ transitions of Eu^{3+}.[14] It is well-known that the observed emission line intensity pattern of Eu^{3+} is a strong function of the symmetry of the lattice site at which the activator ion is located. This is confirmed by our materials because the orthorhombic KGd[Si(CN$_2$)$_4$]:Eu (Figure 9) shows an emission line pattern that is much different from the pattern of the other four materials because they all crystallize in a tetragonal crystal system.

Excitation spectra were recorded upon monitoring of the 592 nm (^{5}D$_0$–^{7}F$_1$) (Figures 10 and 11) or 612 nm (^{5}D$_0$–^{7}F$_2$) emission (Figure 9). They reveal that all materials show two CT bands with a baricenter at around 300 nm and a shoulder at 370 nm. The presence of several CT bands points to the presence of several types of covalent contacts between the activator Eu^{3+} and the tetracyanamidosilicate anions. It is striking that the CT bands are at rather low energy, which points to the ease of oxidation of the anions, which is in line with our expectations. Because the energetic position of the Eu^{3+} CT is

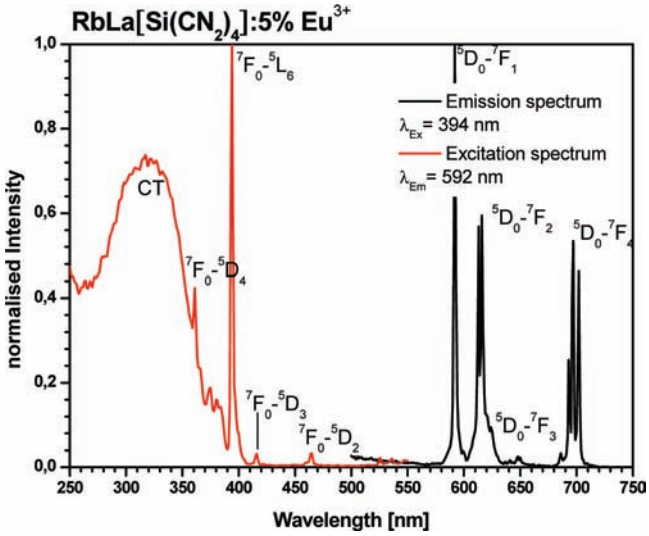

Figure 10. Excitation and emission spectra of $RbLa[Si(CN_2)_4]$:5% Eu^{3+} (tetragonal).

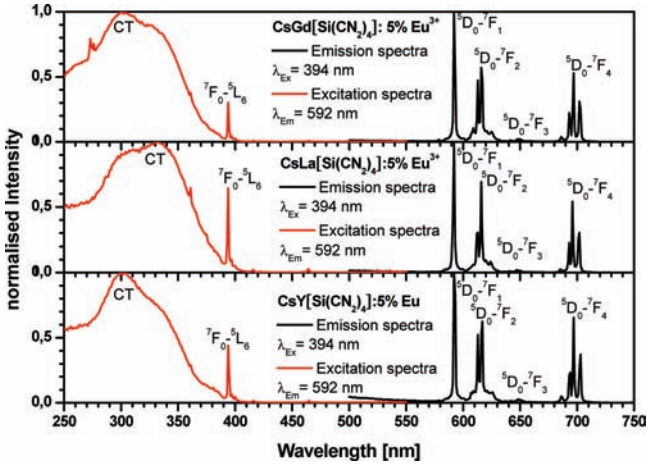

Figure 11. Excitation and emission spectra of $CsRE[Si(CN_2)_4]$:5% Eu^{3+} (RE = Y, La, Gd, all tetragonal).

related to the band gap of a compound,[16] we can estimate the band gap at about 4.5 eV.

Moreover, the excitation spectra of the four tetragonal crystallizing materials show a rather intense excitation line at 394 nm (Figures 10 and 11), which corresponds to the $^7F_0$ to $^5L_6$ transition of Eu^{3+}. A similar observation was made for Eu^{3+}-doped tungstates and molybdates, e.g., in $NaGd(Mo,W)O_4$:Eu.[17] Because of the low energy of the CT transition and the high intensity of the $^7F_0$ to $^5L_6$ transition, Eu^{3+}-activated tetracyanamidosilicates can be useful red-luminescent converter materials for near-UV-emitting LEDs.

Conclusions

In the framework of our research toward novel functional materials, we have synthesized tetracyanamidosilicates of the type $ARE[Si(CN_2)_4]$ with A = K, Rb, and Cs and RE = Y and La−Lu by multilateral solid-state metathesis reactions. In addition to characterization of a series of compounds and elucidation of the crystal structures, we studied their magnetic and luminescence features.

Because the gadolinium compound having the maximal possible number of unpaired electrons per rare-earth cation shows almost perfect Curie paramagnetism typical for a $4f^7$ electron configuration, magnetic ordering cannot be expected for the other rare-earth tetracyanamidosilicates.

Luminescence spectroscopy nicely demonstrated that the cerium-, terbium-, and europium-doped compounds show efficient blue, green, or red luminescence, whereby the observed emission spectra are in line with expectations for compounds activated by Ce^{3+}, Tb^{3+}, and Eu^{3+}, respectively.

The emission line pattern of the europium compounds is clearly governed by the symmetry of the crystal system; i.e., the emission spectrum of the orthorhombic compound $KGd[Si(CN_2)_4]$ is dominated by the $^5D_0-^7F_2$ transition. In contrast, the emission spectra of all compounds crystallizing in the tetragonal crystal system show the most intense line because of a $^5D_0-^7F_1$ transition, which is expected for Eu^{3+} ions located on a dodecahedral crystal site with inversion symmetry.

Excitation spectra of the europium compounds reveal a rather low-lying CT state, which proves the ease of the electron transfer from the alkaline tetracyanamidosilicate anions to the Eu^{3+} ion. This finding is particularly interesting in view of the application of these compounds as radiation converters in near-UV- or blue-emitting InGaN LEDs and justifies our interest in further researching these novel compounds.

Acknowledgment. Support of this research by Deutsche Forschungsgemeinschaft (Bonn) through the project *Nitridocarbonate* is gratefully acknowledged. The authors thank Prof. Dr. Takao Mori, National Institute for Materials Science, Nakami, Japan, for the magnetic measurement.

(16) Dorenbos, P. *J. Lumin.* **2005**, *111*, 89–104.

(17) Neeraj, S.; Kijima, N.; Cheetham, A. K. *Chem. Phys. Lett.* **2004**, *387*, 2–6.